

Vibration analysis of rotating beam with variable cross section using Riccati transfer matrix method

Mahdi Feyzollahzadeh and Mahdi Bamdad*

Mechanical and Mechatronics Engineering, Mechatronic Research Lab, Shahrood University of Technology, Shahrood, Iran

(Received November 16, 2018, Revised February 13, 2019, Accepted February 14, 2019)

Abstract. In this paper, a semi-analytical method will be discussed for free vibration analysis of rotating beams with variable cross sectional area. For this purpose, the rotating beam is discretized through applying the transfer matrix method and assumed the axial force is constant for each element. Then, the transfer matrix is derived based on Euler-Bernoulli's beam differential equation and applying boundary conditions. In the following, the frequencies of the rotating beam with constant and variable cross sections are determined using the transfer matrix method in several case studies. In order to eliminate numerical difficulties in the transfer matrix method, the Riccati transfer matrix is employed for high rotation speed and high modes. The results are compared with the results of the finite elements method and Rayleigh-Ritz method which show good agreement in spite of low computational cost.

Keywords: Riccati; transfer matrix method; rotating beam; cross section; natural frequency

1. Introduction

Recently, rotating flexible beam modelling was important due to its practical uses, such as flexible manipulator arms, compressor and helicopter rotor blades, turbine blades, and so on (Yoo *et al.* 2006). Many researchers have studied the vibrations of these structures due to their importance in the industry. If the functions for axial forces, cross-section and stiffness of beam with variable area are defined, the differential equation of motion will be solved in some cases. Ece *et al.* (2007) provided analytical solution, using exponential functions for cross section and moment of inertia into the beam. Liu and Yeh (1987) used the linear functions for cross section and the moment of inertia and obtained natural frequencies of rotating beam with variable cross section. Banerjee *et al.* (2006) studied vibration of rotating tapered beams using the dynamic stiffness method and Frobenius method. The authors showed that the dynamic stiffness method has some limitations in some taper ratio while provides a solution to these limitations. In another study, the authors examined Coriolis effects on vibrations of rotating beams using the dynamic stiffness method (Banerjee *et al.* 2014).

In particular, solving differential equations of beams with variable cross-sectional area is challenging. Rotating beam leads to create a variable axial force and in certain cases the analytical solution of differential equations would be impossible. Then, researcher for accurate modeling used numerical methods such as FEM (Rao and Gupta 2001, Gunda and Ganguli 2008, Panchore *et al.* 2018, Panchore *et*

al. 2018). It is shown that finite element and numerical methods have an identical specification. In all numerical methods, to increase the accuracy of the results, suitable numbers of elements or steps are needed. Though, once the system size or the number of elements increases, the size of the matrices increases, then the computing time increases too (Kumar and Sankar 1986).

Transfer Matrix Method (TMM) is simple and accurate enough and it is used to analyze the vibration of beams (Lee and Lee 2018, Arici and Granata 2011) and other structures (Chen 2018, Bozdogan and Ozturk 2009). Transfer matrix method has also some advantages in computer implementation (Feyzollahzadeh and Mahmoodi 2016, Li *et al.* 2000, Pestel and Leckie 1963) such as, ease of software design, small memory supplies and obtainability of ready-made transfer matrix catalogues for different elements. On the other hand, in TMM, the accuracy of the results achieved by increasing the number of elements and the determination of the characteristic matrices are not dependent on the number of elements, unlike the numerical methods (Feyzollahzadeh *et al.* 2016). Transfer matrix method is an excellent option for modelling a lot of different systems, particularly those composed of serial connections of elements. A system model can be created by a simple multiplying of the transfer matrices of the individual elements together, and the number of states is added and as a result, using the transfer matrix method can decrease the computational process (Krauss and Okasha 2013). Then it seems that transfer matrix method is appropriate for vibration analysis of the beam with variable cross section. Boiangiu *et al.* (2016) considered the vibration of Euler-Bernoulli beam and determined Transfer matrix for tapered elements by defining a second order function for cross section and fourth order function for the moment of inertia. Al Rjoub and Hamad (2017) discussed

*Corresponding author, Assistant Professor
E-mail: bamdad@shahroodut.ac.ir

free vibration of Euler-Bernoulli and Timoshenko porous beams using transfer matrix method. Although the transfer matrix method has many advantages, it also has some limitations. For instance, in the high modes, transfer matrix method contains numerical difficulties which lead to inaccurate natural frequencies (Pestel and Leckie 1963). Therefore, transfer matrix method is suitable for systems in which low vibration modes are dominant in the design. Also, in many cases when a very stiff spring exists between two elements or in the presence of joint with high flexibility, determination of natural frequencies using the transfer matrix method would be difficult (Pestel and Leckie 1963, Uhrig 1966). In this paper, a semi analytical model is presented for free vibration analysis of rotating beam with variable cross section. For this purpose, the rotating beam is discretized using the transfer matrix method and expanding the Euler-Bernoulli equation. To simplify the equations, it is assumed that the axial force is constant for each element. With this assumption, differential equation of each element can be turned into a differential equation with constant coefficients that can be solved by the separation of variables methods. In this case, the presented model can be used without cross-sections limitation. In order to eliminate numerical difficulties in transfer matrix, Riccati transfer matrix method (RTMM) is used for high rotation speed and high vibration modes. In this case, by using the Riccati transformation, the natural frequencies in the high modes and high rotation speed are easily determined. On the other hand, in the transfer matrix method, the simulation time for free vibrations is proportional to n^2 but it is proportional to $n^2/2$ in the Riccati transfer matrix (Horner and Pilkey 1978). Thus, the dimensions of the matrices are reduced in Riccati transfer matrix. Therefore, the computational cost is reduced compared to the traditional transfer matrix method. Finally, several case studies will be calculated and also the errors of the proposed model will be examined.

2. Equations of motion

Fig. 1 shows the rotating beam with constant rotational speed. Using Euler-Bernoulli beam theory, the free vibration equation of a rotating non-uniform beam can be expressed as (Attarnejad and Shahba 2011)

$$\frac{\partial^2}{\partial x^2} \left(EI(x) \frac{\partial^2 W}{\partial x^2} \right) + \rho A(x) \frac{\partial^2 W}{\partial t^2} - \frac{\partial}{\partial x} \left(T(x) \frac{\partial W}{\partial x} \right) = 0 \quad (1)$$

$$T(x) = \int_x^L \rho A(u) \cdot \Omega^2 \cdot (R + u) du \quad (2)$$

where W is lateral deflection, $EI(x)$ is bending stiffness, ρ is density, $A(x)$ is cross-sectional area, L is beam length, Ω is rotational speed and R is hub radius.

With the solution supposed to $W(x, t) = w(x) \exp(i \omega t)$, the spatial dimension of Eq. (1) is obtained as follows

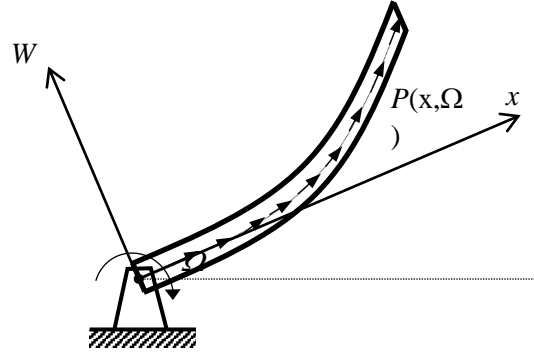


Fig. 1 A view of rotating beam

$$\frac{\partial^2}{\partial x^2} \left(EI(x) \frac{\partial^2 w}{\partial x^2} \right) - \rho A(x) \omega^2 w - \frac{\partial}{\partial x} \left(T(x) \frac{\partial w}{\partial x} \right) = 0 \quad (3)$$

To solve the Eq. (3), it needs to have cross-sectional area and moment of inertia functions along the beam. If the functions of cross sectional area and moment of inertia are determined, the exact solution of Eq. (3) will be obtained in some cases. However, Eq. (3) does not have an exact solution in general. On the other hand, $T(x)$ in Eq. (3) is an integral relationship solution which would be difficult. To provide a comprehensive solution for all forms of cross-section, the transfer matrix method is used in this paper.

3. Applying the transfer matrix method

3.1 Modelling

For modelling by the transfer matrix method, the rotating beam is discretized into n cylindrical continuous beam elements with constant cross-section as shown in Fig. 2. It is assumed that the length of each element x_i is negligible. In this case, the axial force, bending stiffness and the cross section for each element take into account constant and differential equation of motion for each element is transformed as the following

$$EI_i \frac{d^4 v}{d\eta^4} - P_i \frac{d^2 v}{d\eta^2} - \rho A_i \omega^2 \frac{dv}{d\eta} = 0 \quad (4)$$

where, P_i is determined by the discretization of Eq. (2), EI_i and A_i can be considered by average of the points i and $i-1$. In this case, solution of Eq. (4) can be expressed as

$$v(\eta) = C_1 \cosh s_1 \eta + C_2 \sinh s_1 \eta + C_3 \cos s_2 \eta + C_4 \sin s_2 \eta \quad (5)$$

in which

$$s_1^2, s_2^2 = \frac{P_i}{2EI_i} \pm \left(\frac{P_i^2}{(2EI_i)^2} + \frac{\rho A_i \omega^2}{EI_i} \right)^{1/2} \quad (6)$$

3.2 Obtaining the transfer matrix

Concluding from the derivation of dimensional solution, the slope θ , shear force V and moment M for each segment

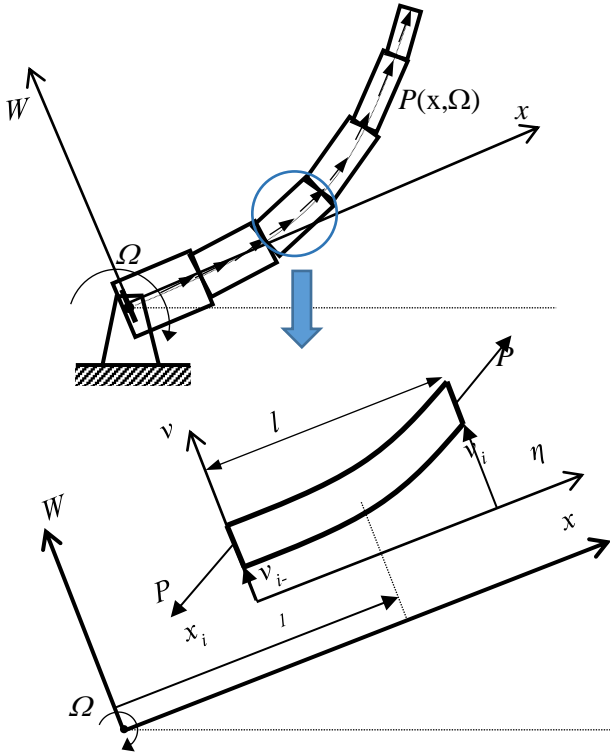


Fig. 2 Discretization of rotating beam applying the TMM

are following

$$\begin{aligned}
 v(\eta) &= C_1 \cosh s_1 \eta + C_2 \sinh s_1 \eta + C_3 \cos s_2 \eta + C_4 \sin s_2 \eta \\
 \theta &= \frac{\partial v}{\partial \eta} = (s_1 \sinh s_1 \eta) C_1 + (s_1 \cosh s_1 \eta) C_2 \\
 &\quad - (s_2 \sin s_2 \eta) C_3 + (s_2 \cos s_2 \eta) C_4 \\
 M &= EI \left(\frac{\partial^2 v}{\partial \eta^2} \right) = (EIs_1^2 \cosh s_1 \eta) C_1 + (EIs_1^2 \sinh s_1 \eta) C_2 \\
 &\quad - (EIs_2^2 \cos s_2 \eta) C_3 - (EIs_2^2 \sin s_2 \eta) C_4 \\
 V &= \frac{\partial M}{\partial \eta} - P \frac{\partial v}{\partial \eta} = [(-P + EIs_1^2) s_1 \sinh s_1 \eta] C_1 \\
 &\quad + [(-P + EIs_1^2) s_1 \cosh s_1 \eta] C_2 \\
 &\quad + [(P + EIs_2^2) s_2 \sin s_2 \eta] C_3 \\
 &\quad - [(P + EIs_2^2) s_2 \cos s_2 \eta] C_4
 \end{aligned} \quad (7)$$

The relations in Eq. (7) can be represented in matrix form as

$$\mathbf{Z}(\eta) = \mathbf{T}(\eta) \cdot \mathbf{C} \quad (8)$$

where $\mathbf{T}(\eta)$ is called transfer matrix function, $\mathbf{z}(\eta)$ is state vector and \mathbf{C} is vector of constants which are obtainable as follows

$$\mathbf{Z}(\eta) = \begin{bmatrix} v \\ \theta \\ M \\ V \end{bmatrix}, \quad \mathbf{C} = \begin{bmatrix} C_1 \\ C_2 \\ C_3 \\ C_4 \end{bmatrix} \quad (9)$$

Fig. 2 shows i th elements. In The point $i-1$, amount of η

equal to zero and the state vector is acquired

$$\mathbf{Z}_{i-1} = \mathbf{T}(\mathbf{0}) \cdot \mathbf{C} \quad (10)$$

and vector \mathbf{C} is

$$\mathbf{C} = \mathbf{T}(\mathbf{0})^{-1} \cdot \mathbf{Z}_{i-1} \quad (11)$$

by inserting vector \mathbf{C} in Eq. (10), the state vector can be obtained as follows

$$\mathbf{Z}(\mathbf{z}) = \mathbf{T}(\eta) \cdot \mathbf{T}(\mathbf{0})^{-1} \cdot \mathbf{Z}_{i-1} \quad (12)$$

In the point i , amount of η equal to l and the state vector is

$$\mathbf{Z}_i = \mathbf{T}(l) \cdot \mathbf{T}(\mathbf{0})^{-1} \cdot \mathbf{Z}_{i-1} = \mathbf{H}_i \cdot \mathbf{Z}_{i-1} \quad (13)$$

herein, \mathbf{H}_i is transfer matrix between two nodes i and $i-1$.

3.3 Applying boundary conditions

Using a recursive relationship in Eq. (13), the state vector between the first point at the support and the end point can be described as follows

$$\mathbf{Z}_n = \mathbf{H}_n \mathbf{H}_{n-1} \mathbf{H}_{n-2} \dots \mathbf{H}_2 \mathbf{H}_1 \mathbf{Z}_1 = \mathbf{H}_t \mathbf{Z}_1 \quad (14)$$

where \mathbf{Z}_n is state vector at the end, \mathbf{Z}_1 is state vector at the support and \mathbf{H}_t is total transfer matrix. At the end of the beam, value of V_n and M_n are equal to zero. If assume that fulcrum is clamped, slope and displacement are equal to zero at the support. In this case the, the relationship between the point l and point n can be obtained as

$$\begin{bmatrix} v \\ \theta \\ 0 \\ 0 \end{bmatrix}_n = \begin{bmatrix} a_{11} & a_{12} & a_{13} & a_{14} \\ a_{21} & a_{22} & a_{23} & a_{24} \\ a_{31} & a_{32} & a_{33} & a_{34} \\ a_{41} & a_{42} & a_{43} & a_{44} \end{bmatrix} \begin{bmatrix} 0 \\ 0 \\ M \\ V \end{bmatrix}_1 \quad (15)$$

for non-zero answer should be zero determinant of the following matrix

$$\Delta\omega = \det \begin{bmatrix} a_{33} & a_{34} \\ a_{43} & a_{44} \end{bmatrix} \quad (16)$$

If assume that fulcrum is hinge joint, the moment and displacement are equal to zero at the base. In this case, the relationship between the point 1 and point n can be obtained as

$$\begin{bmatrix} v \\ \theta \\ 0 \\ 0 \end{bmatrix}_n = \begin{bmatrix} a_{11} & a_{12} & a_{13} & a_{14} \\ a_{21} & a_{22} & a_{23} & a_{24} \\ a_{31} & a_{32} & a_{33} & a_{34} \\ a_{41} & a_{42} & a_{43} & a_{44} \end{bmatrix} \begin{bmatrix} 0 \\ \theta \\ 0 \\ V \end{bmatrix}_1 \quad (17)$$

In a same manner to the previous, $\Delta\omega$ can be obtained as follows

$$\Delta\omega = \det \begin{bmatrix} a_{32} & a_{34} \\ a_{42} & a_{44} \end{bmatrix} \quad (18)$$

$\Delta\omega$ is a function of the natural frequency that by resolve and determination of its roots can be obtained natural frequency of rotating beam.

4. Riccati transfer matrix

4.1 Riccati transformation

To use Riccati transformation, the state vector is divided into two parts

$$\mathbf{Z}_i = [\mathbf{F} \quad \mathbf{E}]^T \quad (19)$$

where \mathbf{F} is $n/2$ state variables that are known on the first point and \mathbf{E} contains $n/2$ state variables that are unknown on the first point. Therefore, Eq. (13) converts as follows

$$\begin{bmatrix} \mathbf{F} \\ \mathbf{E} \end{bmatrix}_i = \begin{bmatrix} \mathbf{U}_{11} & \mathbf{U}_{12} \\ \mathbf{U}_{21} & \mathbf{U}_{22} \end{bmatrix} \begin{bmatrix} \mathbf{F} \\ \mathbf{E} \end{bmatrix}_{i-1} + \begin{bmatrix} \mathbf{F}_f \\ \mathbf{E}_f \end{bmatrix} \quad (20)$$

that \mathbf{F}_f and \mathbf{E}_f represent the external forces in the i th element. The Riccati transformation is defined as

$$\mathbf{F}_i = \mathbf{S}_i \mathbf{E}_i + \mathbf{P}_i \quad (21)$$

By inserting Eq. (21) in Eq. (20), \mathbf{E}_i can be obtained as follows

$$\mathbf{E}_i = (\mathbf{U}_{21} \mathbf{S}_{i-1} + \mathbf{U}_{22}) \mathbf{E}_{i-1} + \mathbf{U}_{21} \mathbf{P}_{i-1} + \mathbf{E}_f \quad (22)$$

By rewriting the Eq. (22), \mathbf{E}_{i-1} is obtained as follows

$$\mathbf{E}_{i-1} = (\mathbf{U}_{21} \mathbf{S}_{i-1} + \mathbf{U}_{22})^{-1} \mathbf{E}_i - (\mathbf{U}_{21} \mathbf{S}_{i-1} + \mathbf{U}_{22})^{-1} (\mathbf{U}_{21} \mathbf{P}_{i-1} + \mathbf{E}_f) \quad (23)$$

\mathbf{T} and \mathbf{Q} are defined as follows (Yu and Hao 2012)

$$\begin{aligned} \mathbf{T}_i &= (\mathbf{U}_{21} \mathbf{S}_{i-1} + \mathbf{U}_{22})^{-1} \\ \mathbf{Q}_i &= -(\mathbf{U}_{21} \mathbf{P}_{i-1} + \mathbf{E}_f) \end{aligned} \quad (24)$$

Therefore, Eq. (21) is represented as follows

$$\mathbf{F}_{i-1} = \mathbf{T}_i \mathbf{E}_i + \mathbf{Q}_i \quad (25)$$

By inserting Eq. (21) and Eq. (25) in Eq. (20), \mathbf{F}_i can be obtained as follows

$$\mathbf{F}_i = \mathbf{U}_{11} [\mathbf{S}_{i-1} (\mathbf{T}_i \mathbf{E}_i + \mathbf{Q}_i) + \mathbf{P}_{i-1}] + \mathbf{U}_{12} (\mathbf{T}_i \mathbf{E}_i + \mathbf{Q}_i) + \mathbf{F}_f \quad (26)$$

By placing Eq. (21) in Eq. (26), the Riccati transfer formulation can be expressed as

$$\begin{aligned} \mathbf{S}_i &= (\mathbf{U}_{11} \mathbf{S}_{i-1} + \mathbf{U}_{12}) \mathbf{T}_i \\ \mathbf{P}_i &= \mathbf{U}_{11} \mathbf{P}_{i-1} + \mathbf{S}_i \mathbf{Q}_i + \mathbf{F}_f \end{aligned} \quad (27)$$

Eq. (27) is the overall recursive relation for determination of \mathbf{S} and \mathbf{P} at each section.

4.2 Applying boundary conditions

To apply the Riccati method, \mathbf{F} and \mathbf{E} must be specified. If the support to be considered as a hinge joint, in this case the bending moment and displacement are equal to zero at the base. In this case, \mathbf{F} and \mathbf{E} are selected as follows

$$\mathbf{F} = \begin{bmatrix} v \\ M \end{bmatrix}, \quad \mathbf{E} = \begin{bmatrix} \theta \\ V \end{bmatrix} \quad (28)$$

On the other hand, if support is clamped, \mathbf{F} and \mathbf{E} are selected as follows

$$\mathbf{F} = \begin{bmatrix} v \\ \theta \end{bmatrix}, \quad \mathbf{E} = \begin{bmatrix} M \\ V \end{bmatrix} \quad (29)$$

Hence, the first point was selected a homogeneous for \mathbf{F} . Thus, the boundary conditions at the first point are obtained as follows

$$\mathbf{F}_0 = [\mathbf{0}] \quad (30)$$

In the free vibrations, value of \mathbf{P} and \mathbf{Q} are equal to zero for all elements. Therefore, from Eq. (21) can be obtained as

$$\mathbf{S}_0 = [\mathbf{0}]_{2 \times 2} \quad (31)$$

Now, the boundary conditions were applied at the end point. At the free end of the beam, value of \mathbf{E}_n is equal to zero. Therefore, Eq. (21) for the end point is obtained as follows

$$\mathbf{F}_n = \mathbf{S}_n \cdot [\mathbf{0}] \quad (32)$$

\mathbf{F}_n is non-zero, therefore, value of \mathbf{S}_n must be zero. Thus $\Delta\omega$ can be determined as

$$\Delta\omega = \det(\mathbf{S}_n^{-1}) \quad (33)$$

5. Results and discussion

5.1 Beam with constant cross section

In order to examine the accuracy of the proposed method, natural frequency of rotating beam is evaluated using the TMM and the results are compared with the results of previous study (Liu and Yeh 1987). In order to make a dimensionless natural frequency, the following equation was used: $\kappa = \rho A \omega^2 L^4 / EI$. Also, to make dimensionless rotating, this equation was applied: $\lambda = \rho A \Omega^2 L^4 / EI$. To determine natural frequencies, a program is prepared in the MATLAB software and results shows in Fig. 3 for $\lambda=2, 6$ and 10 . Using the above diagram can be calculated the natural frequency from the jumping points. Using Fig. 3, first to third natural frequencies of rotating uniform beam are shown in Table 1. To check the sensitivity of the transfer matrix method related to the number of elements, natural frequencies in 2, 5 and 10 element is determined. By examining the values in Table 1, it can be seen that in all the vibration modes, increasing the rotational speed lead to reduced accuracy of the results. On the other hand, sensitivity of the number of elements in high value of rotational speed is more important. For example, for the case $\lambda = 0$ that beam has not rotation, natural frequency values are the same for all three models. This is due to the influence of axial force. The axial force is

Table 1 Comparison of the TMM results with the previous results for the first to third natural frequencies

λ	Present study (TMM)			Liu and Yeh (1987)
	n=2	n=5	n=10	
First natural frequency	0	3.5160	3.5160	3.5160
	2	4.1118	4.1344	4.1366
	4	5.5159	5.5751	5.5826
	6	7.2145	7.3410	7.3558
	8	9.0145	9.2263	9.2497
	10	10.8497	11.1596	11.1928
Second natural frequency	0	22.0345	22.0345	22.0345
	2	22.6967	22.6229	22.6169
	4	24.5649	24.3037	24.2810
	6	27.3621	26.8726	26.8256
	8	30.7953	30.0986	30.0233
	10	34.6369	33.7871	33.6817
Third natural frequency	0	61.6972	61.6972	61.6972
	2	62.3461	62.2835	62.2757
	4	64.2537	64.0078	63.9767
	6	67.3121	66.7751	66.7065
	8	71.3681	70.4527	70.3334
	10	76.2520	74.8948	74.7129

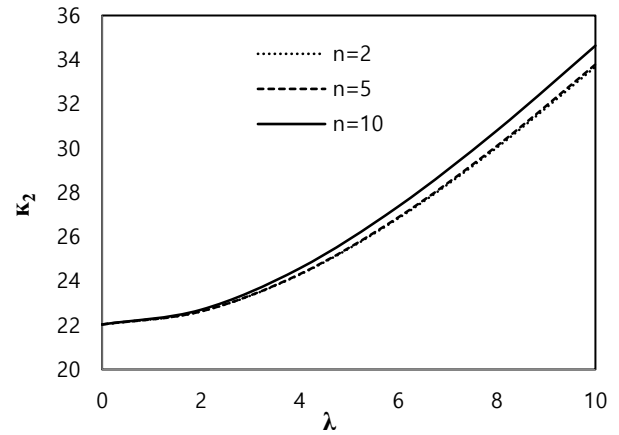


Fig. 5 Second natural frequency changes

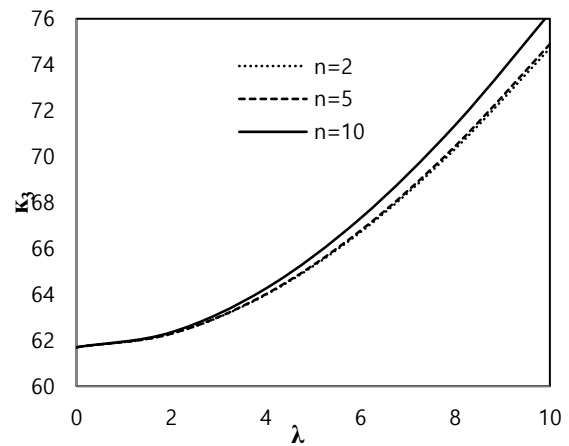


Fig. 6 Third natural frequency changes

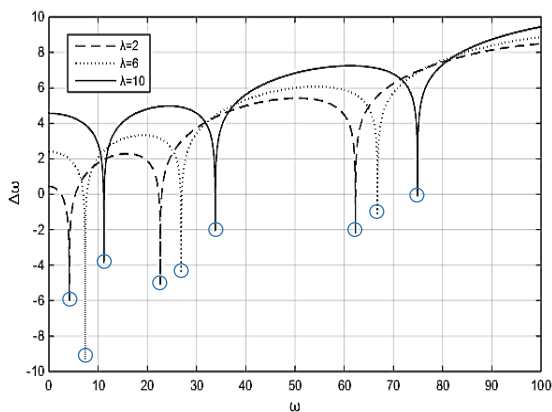


Fig. 3 Logarithm of the $\Delta\omega$ for $\lambda=2, 6$ and 10

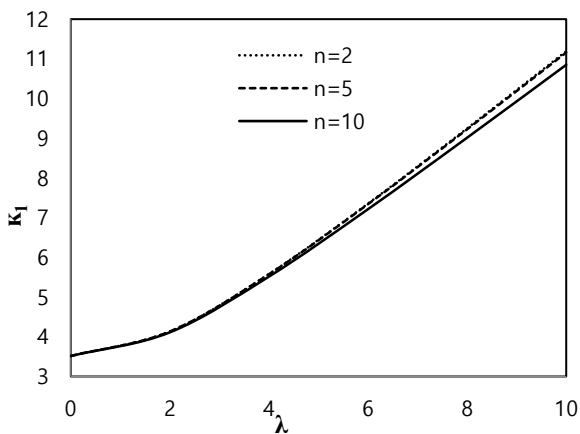


Fig. 4 First natural frequency changes

negligible at low value of rotational speed. Therefore, the low number of elements leads to high accuracy in the results. On the other hand, increasing the rotation speed leads to increase of the axial force and in this case, using the low number of elements leads to decrease accuracy in the results.

In Figs. 4 to 6, the effect of rotational speed variations on the natural frequencies in a number of elements is investigated. For this purpose, in Fig. 4 the first natural frequency, in Fig. 5 the second natural frequency and in Fig. 6, the third natural frequency is presented. By examining the above figures, it can be seen that increase of rotation speed lead to increase the natural frequency in all vibration modes.

For closer look at the effect of the number of elements in the results, error plotting in terms of the number of elements can be useful. This diagram is plotted in Figs. 7-9 for the first to third natural frequencies. By examining the above figures, it can be seen that by increasing the number of the elements, the slope of error for all frequencies has decreased. Then, by increasing the number of elements, the slope is nearly constant. In this case, another error creates in addition error of beam with constant cross-section. In the beam with constant cross section, the only error is error of assuming constant axial force in elements. In beam with

Table 2 Comparison of the TMM results with the previous results for the first to third natural frequencies

λ	Present study (TMM)							Gunda and Ganguli (2008)	Wang and Woreley (2004)	
	n=2	n=5	n=10	n=20	n=40	n=100	n=200			
First natural frequency	0	4.5116	5.1464	5.2414	5.2656	5.2717	5.2734	5.2737	5.2738	5.2738
	2	5.0284	5.5240	5.6306	5.6782	5.7016	5.7155	5.7202	5.7249	5.7249
	5	6.8716	7.1557	7.3220	7.4592	7.5454	7.6032	7.6235	7.6443	7.6443
	10	10.7939	11.0069	11.3600	11.6773	11.8786	12.0135	12.0608	12.1092	12.1092
Second natural frequency	0	20.2111	23.1584	23.7861	23.9491	23.9902	24.0019	24.0035	24.0041	24.0041
	2	20.8055	23.5380	24.1489	24.3236	24.3787	24.4017	24.4077	24.4130	24.4129
	5	23.6030	25.4362	25.9725	26.2036	26.3252	26.4032	26.4303	26.4581	26.4581
	10	30.9605	31.2524	31.6382	32.0315	32.3358	32.5637	32.6481	32.7369	32.7367
Third natural frequency	0	57.0416	57.4092	59.2957	59.7995	59.9273	59.9633	59.9684	59.9702	59.9708
	2	57.5815	57.7831	59.6509	60.1653	60.3054	60.3517	60.3608	60.3670	60.3676
	5	58.3652	59.7055	61.4812	62.0491	62.2510	62.3495	62.3791	62.4070	62.4078
	10	65.3380	66.0867	67.6093	68.3415	68.7350	68.9961	69.0895	69.1852	69.1875

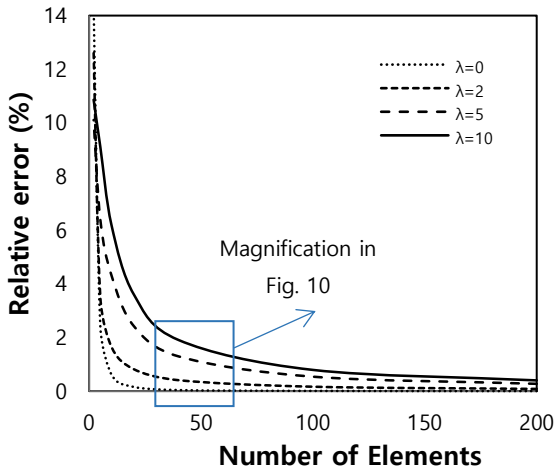


Fig. 7 The relative error in terms of the number of elements for the first natural frequency

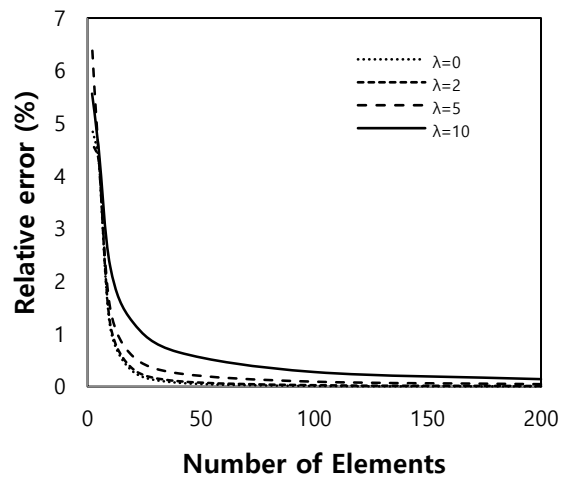


Fig. 9 The relative error in terms of the number of elements for the second natural frequency

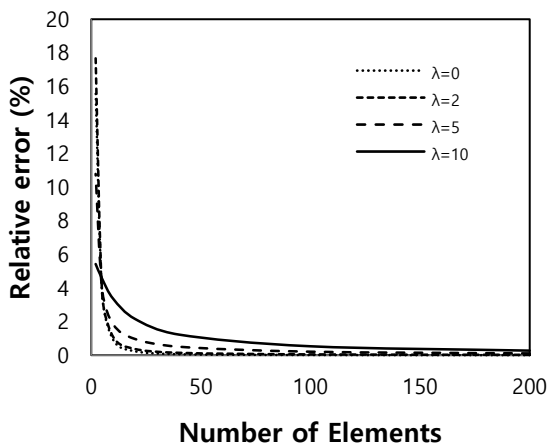
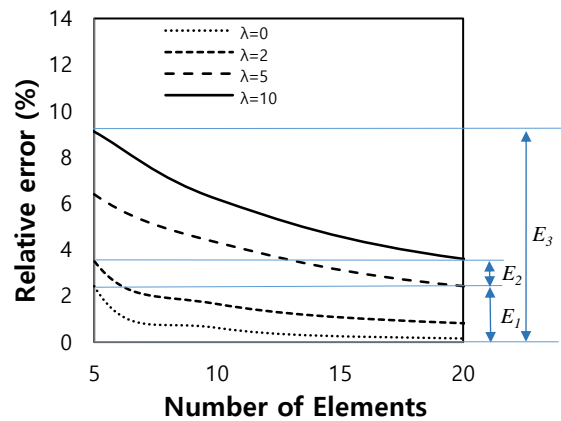


Fig. 8 The relative error in terms of the number of elements for the second natural frequency



E_1 : error of bending stiffness modeling ($\lambda=0, n=5$)
 E_2 : error of axial force modeling ($\lambda=2, n=5$)
 E_3 : error of axial force modeling ($\lambda=10, n=5$)

variable cross section, addition to this error, the bending stiffness modeling error and bending stiffness modeling

Fig. 10 Magnified section of Fig. 7

Table 4 Hardware and software specifications of the used personal computer

Item	Value
OS Name	Microsoft Windows 7 Ultimate
System Model	HP ProBook 4520s
Processor	Intel(R) Core(TM) i5 CPU M 480 @ 2.67 GHz
RAM	4.00 GB
Version	6.1.7601 Service Pack 1 Build 76016
System Type	X86-based PC
Hardware	Version = "6.1.7601.17514"
Available Virtual Memory	4.29 GB

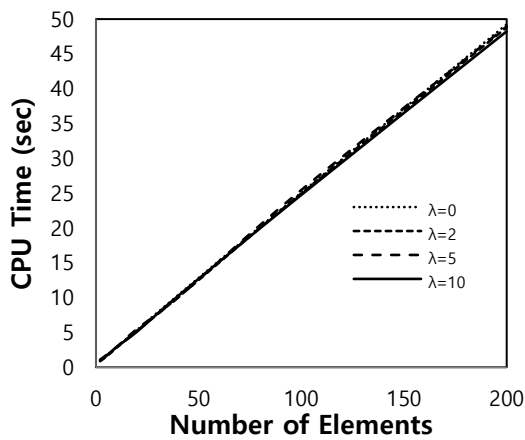


Fig. 11 The simulation time for different number of elements

Table 5 Comparison of the RTMM results with the previous results

λ	FEM (Ganesh and Ganguli 2013)	Rayleigh-Ritz (Ganesh and Ganguli 2013)	Present study (RTMM)
12	14.0313	14.0570	14.0010
50	51.8334	51.8413	51.6010
100	100.8197	100.8237	100.8237

error can also be added in the results. In the discretization of a beam with variable cross section assumed that the cross sectional area and bending stiffness are constant for each element. To clarify this issue, a part of Fig. 7 has been magnified in Fig. 10. It shows that the error rate depends on the number of elements and rotational speed. The axial force is zero for not rotational beam is ($\lambda = 0$) and there is only an error due to bending stiffness modeling. When the number of elements and the rotational speed are small ($\lambda = 2, n = 5$), the bending stiffness of the beam model is very different from the actual value. On the other hand, the amount of axial force is small because the rotational speed is small. Therefore, in this case, the error rate of bending stiffness modeling is greater than the axial force modeling. With increasing the rotational speed ($\lambda = 10, n = 5$), the amount of axial force increases. Hence, the axial force error

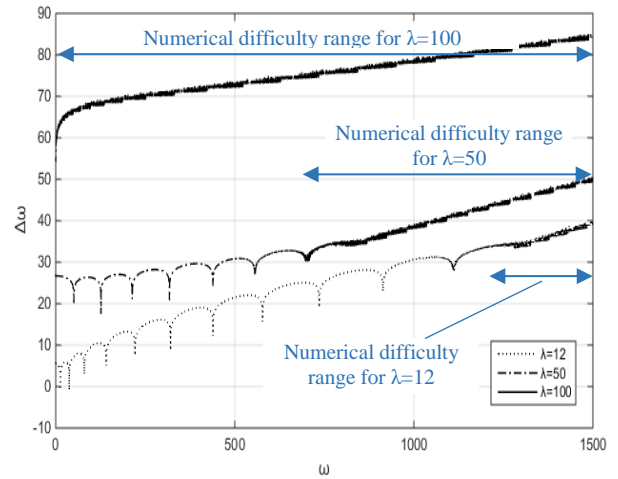


Fig. 12 Logarithm of the $\Delta\omega$ for $\lambda=12, 50$ and 100

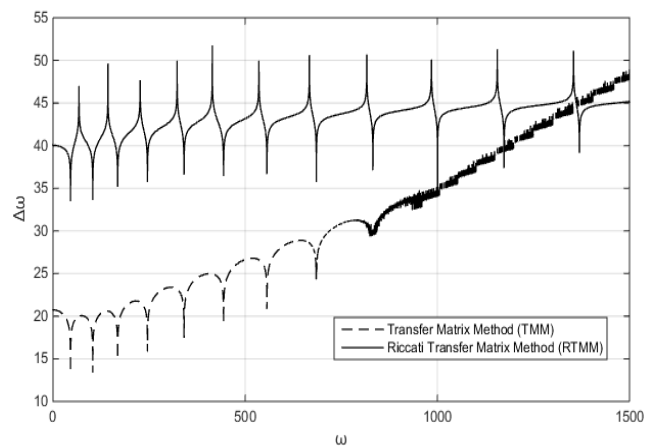


Fig. 13 Comparison of the TMM with RTMM

is greater than the bending stiffness error. Thus, to increase the accuracy, high number of elements at high rotational speed must be applied.

In the following, the effect of number of elements on the simulation time in different rotational speed value is investigated. Table 4 shows the hardware and software specifications of personal computer employed for the analysis. In Fig. 11, the simulation time for different number of elements and different rotational speed is displayed. It can be addressed from above figure that the simulation time is only dependent on the number of elements. On the other hand, the simulation time has a linear relationship with the number of elements. This can be a useful tool for estimating simulation time for optimization algorithms and so on.

Formerly, TMM numerical difficulties are investigated in different rotation speed. For this purpose, three rotation speed ranges including: low rotation speed ($\lambda=12$), normal rotation speed ($\lambda=50$) and high rotation speed ($\lambda=100$) are evaluated (Ganesh and Ganguli 2013). In Fig. 12, logarithm of $\Delta\omega$ is plotted at high frequencies for three rotation speed. By examining Fig. 12 can be obtained that the transfer matrix method leads to numerical difficulties in the high vibration modes. Creation of numerical difficulty is proportional to rotation speed and by increasing the rotation

speed, numerical difficulties is created in lower vibration modes. For instance, the transfer matrix method contains numerical difficulty after the tenth mode for $\lambda = 12$. For $\lambda = 50$, numerical difficulty is created after the sixth mode and for $\lambda=100$, it is not possible to calculate the natural frequency using the transfer matrix method. Therefore, for high rotational speed, or high vibration modes, the transfer matrix method cannot be a suitable method for determining the natural frequencies. In order to solve this problem, the Riccati transfer matrix is used in Fig. 13. For this purpose, in the above figure, logarithm of $\Delta\omega$ for $\lambda=50$ is plotted using TMM and RTMM. Also, the natural frequency in different rotation speeds are determined using the RTMM in Table 5 and the results are compared using previous research (Ganesh and Ganguli 2013). For this purpose, the RTMM results have been compared with the results of the finite element method and Rayleigh-Ritz method in (Ganesh and Ganguli 2013). As it is clear from the Fig. 13 and Table 5, the Riccati transfer matrix has been stable in high modes. Therefore, Riccati transfer matrix can be used to determine the high frequencies in the rotational beams.

6. Conclusions

In this paper, Riccati transfer matrix method was used to free vibration analysis of rotating beam with variable cross section. For this purpose, the Euler-Bernoulli's beam differential equation was used and by applying the boundary conditions, the required equations were obtained for determination of the natural frequencies. The procedure achieved by the presented transfer matrix method is applied in several case studies that results can be categorized as follows:

- Unlike the analytical methods that are applicable to the specific models, the proposed method can be used for rotating beam vibration without cross-sectional area limitation.
- In all vibration modes, with increasing rotational speed the natural frequencies also increase.
- The results of the presented model have two sources of error, including assuming constant axial force and bending stiffness modeling. When the beam is not rotational ($\lambda = 0$), the axial force is zero and there is only an error due to bending stiffness modeling. When the number of elements and the rotational speed are small ($\lambda = 2$, $n = 5$), the bending stiffness of the beam model is very different from the actual value and the amount of axial force is small. Therefore, the error rate of bending stiffness modeling is greater than the axial force modeling. With increasing the rotational speed ($\lambda = 10$, $n = 5$), the amount of axial force increases. Therefore, the axial force error is greater than the bending stiffness error.
- Presented model errors are proportional to the rotational speed and number of elements. Accuracy in the model grows with increasing number of elements. In this case, the determinant of the characteristic equation does not depend on the number of elements unlike the numerical methods such as FEM. Therefore, with increasing elements number, the simulation time does not significantly grows.

On the other hand, by using Riccati transformation, the dimensions of the matrices are reduced. Therefore, the simulation time is reduced compared to the traditional transfer matrix method. As an example for a case study, by selecting 50 elements, the simulation time was about 15 seconds and with the selection of 200 elements, the simulation time was about 50 seconds.

- Riccati transfer matrix has been stable in high vibration modes and therefore, it can be used to determine the natural frequencies in high rotational speed. As an example for a case study, the transfer matrix method contains numerical difficulty after the tenth mode for $\lambda = 12$. For $\lambda = 50$, numerical difficulty is created after the sixth mode and for $\lambda=100$, it is not actually possible to calculate the natural frequency. As a result, Riccati transfer matrix can be employed to determine the natural frequencies without rotational speed limitations.

References

- Al Rjoub, Y.S. and Hamad, A.G. (2017), "Free vibration of functionally Euler-Bernoulli and Timoshenko graded porous beams using the transfer matrix method", *KSCE J. Civil Eng.*, **21**(3), 792-806.
- Arici, M. and Granata, M.F. (2011), "Generalized curved beam on elastic foundation solved by transfer matrix method", *Struct. Eng. Mech.*, **40**(2), 279-295.
- Attarnejad, R. and Shahba, A. (2011), "Dynamic basic displacement functions in free vibration analysis of centrifugally stiffened tapered beams; a mechanical solution", *Meccan.*, **46**(6), 1267-1281.
- Banerjee, J. and Kennedy, D. (2014), "Dynamic stiffness method for inplane free vibration of rotating beams including Coriolis effects", *J. Sound Vibr.*, **333**(26), 7299-7312.
- Banerjee, J., Su, H. and Jackson, D. (2006), "Free vibration of rotating tapered beams using the dynamic stiffness method", *J. Sound Vibr.*, **298**(4-5), 1034-1054.
- Boiangiu, M., Ceausu, V. and Untaroiu, C.D. (2016), "A transfer matrix method for free vibration analysis of Euler-Bernoulli beams with variable cross section", *J. Vibr. Contr.*, **22**(11), 2591-2602.
- Bozdogan, K.B. and Ozturk, D. (2009), "Vibration analysis of asymmetric shear wall and thin walled open section structures using transfer matrix method", *Struct. Eng. Mech.*, **33**(1), 95-107.
- Chen, Y. (2018), "Transfer matrix method for solution of FGMs thick-walled cylinder with arbitrary inhomogeneous elastic response", *Smart Struct. Syst.*, **21**(4), 469-477.
- Ece, M.C., Aydogdu, M. and Taskin, V. (2007), "Vibration of a variable cross-section beam", *Mech. Res. Commun.*, **34**(1), 78-84.
- Feyzollahzadeh, M. and Mahmoodi, M. (2016), "Dynamic analysis of offshore wind turbine towers with fixed monopile platform using the transfer matrix method", *J. Sol. Mech.*, **8**(1), 130-151.
- Feyzollahzadeh, M., Mahmoodi, M., Yadavar-Nikraves, S. and Jamali, J. (2016), "Wind load response of offshore wind turbine towers with fixed monopile platform", *J. Wind Eng. Industr. Aerodyn.*, **158**, 122-138.
- Ganesh, R. and Ganguli, R. (2013), "Stiff string approximations in Rayleigh-Ritz method for rotating beams", *Appl. Math. Comput.*, **219**(17), 9282-9295.
- Gunda, J.B. and Ganguli, R. (2008), "New rational interpolation functions for finite element analysis of rotating beams", *Int. J.*

- Mech. Sci.*, **50**(3), 578-588.
- Horner, G. and Pilkey, W. (1978) "The Riccati transfer matrix method", *J. Mech. Des.*, **100**(2), 297-302.
- Krauss, R. and Okasha, M. (2013), "Discrete-time transfer matrix modeling of flexible robots under feedback control", *Proceedings of the American Control Conference*, Washington, U.S.A., June.
- Kumar, A.S. and Sankar, T. (1986), "A new transfer matrix method for response analysis of large dynamic systems", *Comput. Struct.*, **23**(4), 545-552.
- Lee, J.W. and Lee, J.Y. (2018), "A transfer matrix method for in-plane bending vibrations of tapered beams with axial force and multiple edge cracks", *Struct. Eng. Mech.*, **66**(1), 125-138.
- Li, Q., Fang, J. and Jeary, A. (2000), "Free vibration analysis of cantilevered tall structures under various axial loads", *Eng. Struct.*, **22**(5), 525-534.
- Liu, W. and Yeh, F.H. (1987), "Vibrations of non-uniform rotating beams", *J. Sound Vibr.*, **119**, 379-384.
- Panchore, V. and Ganguli, R. (2018), "Quadratic B-spline finite element method for a rotating nonuniform Euler-Bernoulli beam", *Int. J. Comput. Meth. Eng. Sci. Mech.*, **19**(5), 340-350.
- Panchore, V., Ganguli, R. and Omkar, S.N. (2018), "Meshfree Galerkin method for a rotating Euler-Bernoulli beam", *Int. J. Comput. Meth. Eng. Sci. Mech.*, **19**(1), 11-21.
- Pestel, E. and Leckie, F.A. (1963), *Matrix Methods in Elastomechanics*, McGraw-Hill.
- Rao, S.S. and Gupta, R. (2001), "Finite element vibration analysis of rotating Timoshenko beams", *J. Sound Vibr.*, **242**(1), 103-124.
- Uhrig, R. (1966), "The transfer matrix method seen as one method of structural analysis among others", *J. Sound Vibr.*, **4**(2), 136-148.
- Wang, G. and Wereley, N.M. (2004), "Free vibration analysis of rotating blades with uniform tapers", *AIAA J.*, **42**(12), 2429-2437.
- Yoo, H.H., Cho, J.E. and Chung, J. (2006), "Modal analysis and shape optimization of rotating cantilever beams", *J. Sound Vibr.*, **290**(1-2), 223-241.
- Yu, A. and Hao, Y. (2012), "Improved Riccati transfer matrix method for free vibration of non-cylindrical helical springs including warping", *Shock Vibr.*, **19**(6), 1167-1180.